DOI: 10.1021/ic9021432

Inorganic Chemistry
Article

Synthetic, Cyclic Voltammetric, Structural, EPR, and UV−Vis Spectroscopic Studies of Thienyl-Containing *meso*-A_2B-cor(Cr^V=O) Systems: Consideration of Three Interrelated Molecular Detection Modalities

Olga A. Egorova,[†,‡] Olga G. Tsay,[†,‡] Snehadrinarayan Khatua,[†,‡] Bhupal Meka,[†,‡,§] Nilkamal Maiti,[†,‡,⊥] Min-Kyu Kim,[¶] Seong Jung Kwon,[‡] Jung Oh Huh,[‡] Daniela Bucella,[∥] Sa-Ouk Kang,[¶] Juhyoun Kwak,[‡] and David G. Churchill*[,†,‡]

[†] *Molecular Logic Gate Laboratory,* [‡] *Department of Chemistry, and School of Molecular Science (BK 21), Korea Advanced Institute of Science and Technology (KAIST), 373-1 Guseong-dong, Yuseong-gu, Daejeon 305-701, Republic of Korea,* [¶] *School of Biological Sciences, Seoul National University, Seoul, Korea, and* [∥] *Department of Chemistry, Columbia University, 3000 Broadway, New York, New York 10027.* [§] *Former BK-21 postdoctoral fellow in the laboratory of D. G. Churchill. Current address: Suven Life Sciences Ltd., Jeedimetla, Hyderabad 500055, India.* [⊥] *Former BK-21 postdoctoral fellow in the laboratory of D. G. Churchill. Current address: Department of Chemistry, Midnapore College, Midnapore 721101, West Bengal, India.*

Received July 30, 2009

We report eight new A_2B-type (M^{n+}) corrolate compounds (two structural studies) that include the oxo[5,15-bis(pentafluorophenyl)-10-R-corrolatochromium(V)] [R = 2-/3-thienyl (**1a**/**2a**), 3-thianaphthyl (**3a**)] species. The first examples of *meso*-A_2 (thienyl)- and Cr-A_2B-corrole types are represented herein. Characterization includes cyclic voltammetry, electron paramagnetic resonance, 2D (^{1}H and ^{13}C) NMR, and UV−vis spectroscopy, mass spectrometry, and elemental analysis. Compounds **1a**−**3a** have enabled analyte binding capacity studies. [Cu^{2+}···O=Cr(cor)] binding represents a new selective mode of corrole-based detection, whereas free-base A_2B-corroles exhibited limited M^{n+} selectivity. The 10-position substitution affects optical profiles in analyte titrations. A limited amount of PPh_3 O-atom uptake from [O=Cr(cor)] was also demonstrated.

Introduction

Corrolate (cor) systems, especially A_3-tris(pentafluorophenyl)corrole- or (tpf)cor-based ones, are, by now, relatively well-known ligands, with many reports relating to metal-mediated catalysis.[1a] This foray has reaped various related ligands and metal complex derivatives alike, as well as subsequent metal-based axial ligands (e.g., M=O, M=N−R), which, in corrole chemistry, possess properties and reactivities that, unlike in the porphyrin literature, are still being studied and established. The terminal oxo and closely related derivatives are of great research interest as potential motifs in "compound I" modeling with small molecules. It is clear that while there continues to be vigorous interest in further exploring the reactive biorelevant porphyrinoid-type axial site chemistry, there may be possibilities other than those catalytic for such derivatives. In this paper, we have synthesized new A_2B-corroles[1b] and report novel Cr=O species. Importantly, we endeavor to expand the potential of these contracted porphyrins as possible useful solution-based polypyrrolic probes through considerations of the interrelationships of the free base, the metal complex, and the terminal oxo derivative.

We propose that the limited number of corrole-based molecular detection systems reflected previously in the literature can now be grouped conveniently into interrelated types as provided in Scheme 1: "Type I", or cavity-centered detection (metallations/protonations), includes chemical

*To whom correspondence should be addressed. E-mail: dchurchill@kaist.ac.kr. Tel.: +82-42-350-2845. Fax: +82-42-350-2810.

(1) (a) Aviv, I.; Gross, Z. *Chem. Commun.* **2007**, 1987. (b) Alemayehu, A. B.; Gonzalez, E.; Hansen, L. K.; Ghosh, A. *Inorg. Chem.* **2009**, *48*, 7794–7799. (c) Meier-Callahan, A. E.; Di Bilio, A. J.; Simkhovich, L.; Mahammed, A.; Goldberg, I.; Gray, H. B.; Gross, Z. *Inorg. Chem.* **2001**, *40*, 6788–6793. (d) For an excellent review of valence and related concepts, see:Parkin, G. *J. Chem. Educ.* **2006**, *83*, 791–799. (e) Czernuszewicz, R. S.; Mody, V.; Czader, A.; Galezowski, M.; Gryko, D. T. *J. Am. Chem. Soc.* **2009**, *131*, 14214–14215.

(2) He, C.-L.; Ren, F.-L.; Zhang, X.-B.; Han, Z.-X. *Talanta* **2006**, *70*, 364–369.

(3) Zhang, X.-B.; Han, Z.-X.; Fang, Z.-H.; Shen, G.-L.; Yu, R.-Q. *Anal. Chim. Acta* **2006**, *562*, 210–215.

(4) (a) Li, C. Y.; Zhang, X. B.; Han, Z. X.; Akermark, B.; Sun, L. C.; Shen, G. L.; Yu, R. Q. *Analyst* **2006**, *131*, 388–393. (b) For a resource for collaborating with Chinese chemical colleagues, see: Chao, H.-Y.; Churchill, D. G. *J. Chem. Educ.* **2008**, *85*, 1210.

(5) Radecki, J.; Dehaen, W. *Comb. Chem. High Throughput Screening* **2006**, *9*, 399–406.

 Published on Web 12/17/2009

Scheme 1. Modes of Analyte Detection Previously Reported and Presented Here, Shown Schematically for a Tri-Meso-Substituted Corrolate System

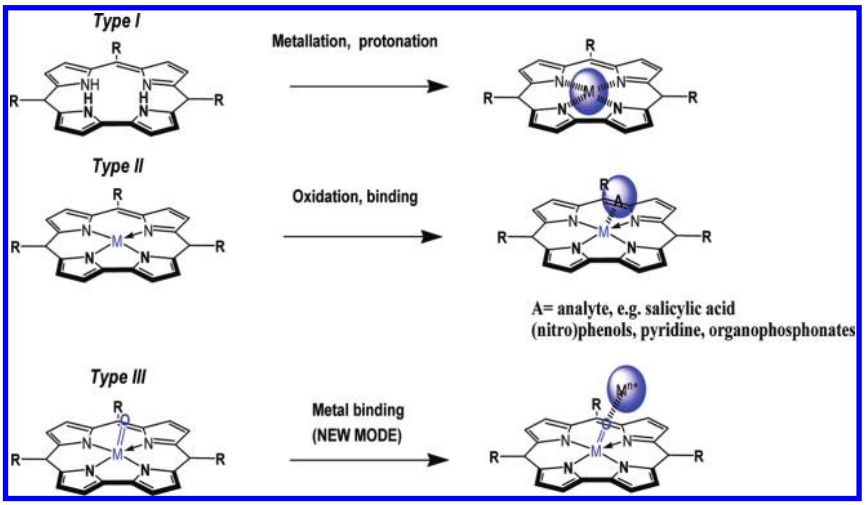

sensing of (metal) cations, such as Hg^{2+},[2] Ag^{+},[3] and, of course, H^{+}.[4−6] "Type II", or Lewis base analyte binding involves (i) volatile analytes[7−12] such as CO,[11,12] (ii) anions, e.g., salicylate/salicylic acid,[13] and (iii) neutral binding molecules such as (nitro)phenolic species,[5] pyridine,[11,12] and organophosphonates.[14] The *meso*-C_6H_5,[2,3] A_3,[9,10] and A_2B types,[8−10,4,13] β-substituted[7,10−12] and (2,17-di)-sulfonated versions,[6] have been represented to date. The spectroscopic sensing mode in these reports is, e.g., fluorescence,[2,6] UV−vis absorption,[11,12,14] and IR.[10] Potentiometry[13,5] has also been featured, along with electrochemical speciation,[13−15] having been pursued elegantly by, e.g., Kadish and co-workers.[11,12] More intricate corrole-based designs such as bis-corroles and linked porphyrin/corrole systems highlight that there is still much latitude in continued exploits in molecular sensing with corroles.[11] "Type III", or oxo-ligand-mediated binding interactions, can first be considered seriously herein because of their growing prevalence and simplicity (i.e., the M═O group). These derivatives are often prepared for/from O-atom transfer. In this potential sensing platform, which would be akin to "Fe−O−Fe"-type dimers,[16] it would be important to avoid derailment of metal ion sensing by, e.g., PR_3 and SR_2 atoms or via olefin oxidation.[17] In real sensing matrixes, the rigorous absence of these substrates may be difficult, however, but a less reactive oxide could be prepared from peripheral porphyrinoid modifications that would involve tuning via the incorporation of various meso groups (vide infra).

In this report, we detail the synthesis and characterization of eight new A_2B-type (M^{n+}) corrolate compounds that include oxo[5,15-bis(pentafluorophenyl)-10-R-corrolatochromium(V)] [R = 2-/3-thienyl (**1a**/**2a**), 3-thianaphthyl (**3a**)]. These derivatives represent the first examples of *meso*-A_2 (thienyl)- and Cr-A_2B-corrole types. The formal replacement of one $-C_6F_5$ group with one thienyl substitution[18,19] was expected to change the extreme electron-withdrawing nature known for the tris-C_6F_5-A_3-type tpf(cor) species. This thienyl substitution also allows for an adjacent ligand-based oxidation site at the sulfur. Chromium was selected for incorporation because of its redox utility. The first synthesis, full characterization, and detailed research on a chromium A_3-triarylcorrolate were performed by Meier-Callahan and co-workers.[20] Our research laboratory has also recently reported a thienyl-containing ABC-type Cr═O derivative.[18e] The structures of compounds have been characterized by a number of physical methods including UV−vis, 2D (^{1}H and ^{13}C) NMR, electron paramagnetic resonance (EPR) spectroscopy, mass spectrometry, elemental analysis, and cyclic voltammetry (CV). Also, two single-crystal X-ray crystallographic studies were performed, in addition to obtaining a measure of the catalytic reactivity of the new corroles. Interestingly, complexes **1a**−**3a** represent type III corrole-based detection platforms for the copper(II) ion.

Experimental Section

Materials and Physical Measurements. All chemicals (e.g., 2-/3-thiophene carboxaldehyde, benzo[*b*]thiophene-3-carboxaldehyde, copper(II) acetate monohydrate, chromium hexacarbonyl,

(6) Mahammed, A.; Weaver, J. J.; Gray, H. B.; Abdelas, M.; Gross, Z. *Tetrahedron Lett*. **2003**, *44*, 2077–2079.
(7) Di Natale, C.; Goletti, C.; Paolesse, R.; Drago, M.; Macagnano, A.; Mantini, A.; Troitsky, V. I.; Berzina, T. S.; Cocco, M.; D'Amico, A. *Sens. Actuators, B* **1999**, *B57*, 183.
(8) Barbe, J.-M.; Canard, G.; Brandès, S.; Guilard, R. *Angew. Chem., Int. Ed*. **2005**, *44*, 3103–3106.
(9) Barbe, J. M.; Canard, G.; Brandes, S.; Guilard, R. *Eur. J. Org. Chem*. **2005**, 4601–4611.
(10) Barbe, J.-M.; Canard, G.; Brandés, S.; Jérôme, F.; Dubois, G.; Guilard, R. *Dalton Trans*. **2004**, 1208–1214.
(11) Kadish, K. M.; Ou, Z. P.; Shao, J. G.; Gros, C. P.; Barbe, J. M.; Jerome, F.; Bolze, F.; Burdet, F.; Guilard, R. *Inorg. Chem*. **2002**, *41*, 3990–4005.
(12) Guilard, R.; Gros, C. P.; Bolze, F.; Jerome, F.; Ou, Z. P.; Shao, J. G.; Fischer, J.; Weiss, R.; Kadish, K. M. *Inorg. Chem*. **2001**, *40*, 4845–4855.
(13) Radecki, J.; Wona, S. T. A.; Eddy, D. B.; Dehaen, W. *Electrochim. Acta* **2006**, *51*, 2282–2288.
(14) Kim, K.; Kim, I.; Maiti, N.; Kwon, S. J.; Bucella, D.; Egorova, O. A.; Lee, Y. S.; Kwak, J.; Churchill, D. G. *Polyhedron* **2009**, *28*, 2418–2430.
(15) Radecki, J.; Stenka, I.; Dolusic, E.; Dehaen, W.; Plavec, J. *Comb. Chem. High Throughput Screening* **2004**, *7*, 375–381.
(16) Harischandra, D. N.; Lowery, G.; Zhang, R.; Newcomb, M. *Org. Lett*. **2009**, *11*, 2089–2092.
(17) Liu, H.-Y.; Yam, F.; Xie, Y.-T.; Li, X.-Y.; Chang, C. K. *J. Am. Chem. Soc*. **2009**, *131*, 12890–12891.
(18) (a) Maiti, N.; Lee, J.; Do, Y.; Shin, H. S.; Churchill, D. G. *J. Chem. Crystallogr*. **2005**, *35*, 949–955. (b) Maiti, N.; Lee, J. S.; Kwon, S. J.; Kwak, J.; Do, Y.; Churchill, D. G. *Polyhedron* **2006**, *25*, 1519–1530. (c) Churchill, D. G.; Maiti, N.; Choi, S. H. Repub. Korean Kongkae Taeho Kongbo KR 2007049466, **2007**. (d) Maiti, N.; Kim, K.; Meka, B.; Churchill, D. G. Unpublished results, **2005**−**2007**. (e) Egorova, O. A.; Tsay, O. G.; Khatua, S.; Huh, J. O.; Churchill, D. G. *Inorg. Chem*. **2009**, *48*, 4634–4636.
(19) Choi, S. H.; Pang, K.; Kim, K.; Jeon, J.; Meka, B.; Bucella, D.; Pang, K.; Khatua, S.; Lee, J.; Churchill, D. G. *Inorg. Chem*. **2008**, *47*, 11071–11083.
(20) Meier-Callahan, A. E.; Gray, H. B.; Gross, Z. *Inorg. Chem*. **2000**, *39*, 3605–3607.

CH_2Cl_2, chloroform, hexane, toluene, and M^{n+} perchlorates) used herein were of analytical grade and were used as received from commercial suppliers (Aldrich, TCI and Junsei chemical companies) except for pyrrole. Pyrrole was distilled over CaH_2 under vacuum prior to use. Plates for thin-layer chromatography (TLC) were cut from the original plates (20 × 20 cm, 60 F silica gel, Merck Co.). A Vilber Lourmat-4LC UV lamp (4 W, 365 nm, 50/60 Hz) was used to probe the fluorescence of reaction "spots" assayed by TLC. The silica gel used in column chromatography was of diameter 0.04−0.063 mm. The silica gel used for dry-column vacuum chromatography was of diameter 0.015−0.040 mm (Merck). All solvents used in NMR spectral analyses were purchased commercially and were of spectroscopy grade. 1D ^{1}H and ^{13}C NMR spectra and 2D COSY, NOESY, HMBC, and HMQC NMR spectra were measured on a Bruker Avance 400 MHz spectrometer with tetramethylsilane used as the internal standard. Elemental analyses of samples were obtained by using a Vario EL III elemental analyzer. UV spectra were recorded with a Jasco V-503 UV−vis spectrometer (1000 nm/min). Emission spectra were obtained using a Shimadzu RF-5310 pc spectrofluorophotometer. EPR spectra were obtained on a Bruker EMX ER 082 spectrometer. High-resolution MALDI-TOF mass spectrometry was performed on an Applied Biosystem Voyager 4394 (ionization method, N_2 laser (337 nm, 3 ns pulse): analyzer 2.0 m linear mode; 3.0 reflector mode.) CV was carried out with a BAS 100B instrument (Bioanalytical Systems, Inc.) under ambient conditions. A three-electrode system was used and consisted of a gold disk working electrode, a platinum wire counter electrode, and an Ag/Ag^+ electrode (MF-2026 kit, Bioanalytical Systems, Inc.) as the reference electrode. The Ag/Ag^+ electrode contained 0.1 M tetrabutylammonium perchlorate (TBAP) and 0.01 M $AgNO_3$ in acetonitrile. In 0.1 M TBAP, $E_{1/2}$ of the ferrocene/ferrocenium ion couple was taken to be 0.13 V vs Ag/Ag^+ in acetonitrile. The values in electrochemical experiments are reported versus the ferrocene/ferrocenium ion redox couple.

General Procedure for the Preparation of Free-Base *meso*-A_2B-*trans*-corroles Starting from 5-(Pentafluorophenyl)dipyrromethane. The details for the synthesis of 5-(pentafluorophenyl) dipyrromethane have been reported previously.[21] Sample of 5-(pentafluorophenyl)dipyrromethane[22a] (1.00 g, 3.20 mmol) and aldehyde (1.60 mmol) were dissolved in a mixed solution of trifluoroacetic acid (1.3 mM)/CH_2Cl_2 (100 mL). The reaction mixture was stirred under nitrogen and left at room temperature. After ~5 h, a portion of dichlorodicyanoquinone (DDQ; 0.726 g, 3.20 mmol) was added dropwise as a toluene (10 mL) solution; the reaction mixture was stirred at room temperature for a further 15 min. Then, the reaction mixture was purified as described below.

Synthesis of 5,15-Bis(pentafluorophenyl)-10-(2-thienyl)corrole, [2THC] (1). The reaction mixture was filtered through a silica pad (CH_2Cl_2) and evaporated. Subsequent dry-column vacuum chromatography (silica, CH_2Cl_2/hexane, 0.7:1.0) afforded pure corrole (113 mg, ca. 10%), which was recrystallized (hexane/CH_2Cl_2, 1:1 by volume) to give dark-purple crystals. ^{1}H NMR (CD_2Cl_2): δ 7.52 (dd, $^3J_{H-H}$ = 5.2 and 3.4 Hz, 1H_c), 7.87 (dd, $^3J_{H-H}$ = 5.36 Hz, $^4J_{H-H}$ = 1.04 Hz, H_d), 7.90 (dd, $^3J_{H-H}$ = 3.46 Hz, $^4J_{H-H}$ = 1.08 Hz, H_b), 8.59 (d, $^3J_{H-H}$ = 3.85 Hz, H_3 and H_{17}), 8.75 (d, $^3J_{H-H}$ = 4.68 Hz, H_7 and H_{13}), 8.91 (d, $^3J_{H-H}$ = 4.77 Hz, H_8 and H_{12}), 9.14 (d, $^3J_{H-H}$ = 4.27 Hz, H_2 and H_{18}). ^{13}C NMR (CD_2Cl_2): δ 147.8 (s), 145.3 (s), 142.9 (s, 1$C_{a\ or\ 10}$), 140.9 (br), 139.5 (m), 137.2 (br), 133.5 (s, 1C_b), 131.5 (br), 128.4 (s, 1C_d), 128.0 (s, C_8 and C_{12}), 127.0 (s, C_e), 126.1 (s, C_7 and C_{13}), 121.6 (br, C_3 and C_{17}), 117.9 (s, C_2 and C_{18}), 114.3 (tr), 104.9 (s, C_9 and C_{11}). MALDI-TOF (M + H^+): m/z 712.56 (calcd), 713.36 (obsd). Anal. Calcd for $C_{35}H_{14}N_4SF_{10}$: C, 58.99; H, 1.98; N, 7.86; S, 4.50. Found: C, 58.90; H, 1.98; N, 7.72; S, 4.45. λ_{abs} (CH_2Cl_2, log ε = 5.2) = 415 nm. Φ_F = 0.003.[23]

Synthesis of 5,15-Bis(pentafluorophenyl)-10-(3-thienyl)corrole, [3THC] (2). The reaction mixture was filtered through a silica pad (CH_2Cl_2). After solvent evaporation, subsequent dry-column vacuum chromatography (silica, CH_2Cl_2/hexane, 1:1) gave a pink-violet band, which contains corrole as well as traces of porphyrin. Recrystallization from *n*-hexane/$CHCl_3$ afforded pure corrole (40 mg, ca. 4.5%) as a purple solid. ^{1}H NMR (CD_2Cl_2): δ 7.77 (dd, $^3J_{H-H}$ = 4.85 and 3.02 Hz, H_c), 7.98 (dd, $^3J_{H-H}$ = 4.81 Hz, $^4J_{H-H}$ = 0.83 Hz, H_b), 8.05 (dd, $^3J_{H-H}$ = 2.72 Hz, $^4J_{H-H}$ = 0.95 Hz, H_d), 8.60 (d, $^3J_{H-H}$ = 4.18 Hz, H_3 and H_{17}), 8.76 (d, $^3J_{H-H}$ = 4.76 Hz, H_7 and H_{13}), 8.86 (d, $^3J_{H-H}$ = 4.75 Hz, H_8 and H_{12}), 9.14 (d, $^3J_{H-H}$ = 4.27 Hz, H_2 and H_{18}). ^{13}C NMR (CD_2Cl_2): δ 147.8 (s), 145.3 (s), 143.4 (br), 141.9 (s, $C_{a\ or\ 10}$), 140.3 (br), 139.6 (m), 137.1 (m), 135.8 (br), 134.4 (s, C_b), 132.0 (br), 128.6 (s, C_d), 127.9 (s, C_8 and C_{12}), 125.8 (s, C_7 and C_{13}), 124.6 (s, C_e), 122.2 (br), 118.0 (s, C_2 and C_{18}), 114.4 (t), 108.0 (s), 96.9 (br). MALDI-TOF (M + H^+): m/z 712.56 (calcd), 713.37 (obsd). Anal. Calcd for $C_{35}H_{14}N_4SF_{10}$: C, 58.99; H, 1.98; N, 7.86; S, 4.50. Found: C, 59.80; H, 2.10; N, 7.92; S, 4.53. λ_{abs} (CH_2Cl_2, log ε = 5.1) = 416 nm. Φ_F = 0.004 (this is time-dependent: vide infra).

Synthesis of 5,15-Bis(pentafluorophenyl)-10-(3-thianaphthyl)-corrole, [TNPC] (3). The reaction mixture was filtered through a pad of silica gel (CH_2Cl_2). After solvent evaporation, corrole purification was carried out by using dry-column vacuum chromatography (CH_2Cl_2/hexane, 0.7:1.0), and a green-violet band exhibiting red fluorescence was collected. Subsequent recrystallization from hexane/CH_2Cl_2 afforded a pure purple solid compound (**3**). Yield: 76 mg, ca. 7%. ^{1}H NMR ($CDCl_3$): δ 7.51 (m, H_e and H_f), 8.02 (m, H_d and H_g), 8.30 (s, H_b), 8.53 (d, $^3J_{H-H}$ = 2.18 Hz, H_3 and H_{17}), 8.71 (d, $^3J_{H-H}$ = 4.47 Hz, H_7 and H_{13}), 8.98 (d, $^3J_{H-H}$ = 4.68 Hz, H_8 and H_{12}), 9.03 (d, $^3J_{H-H}$ = 4.02 Hz, H_2 and H_{18}). ^{13}C NMR ($CDCl_3$): δ 147.35 (br, s), 144.9 (m), 143.1 (br, C_{PFP}), 142.9 (s, $C_{a\ or\ 10}$), 142.0 (s, C_{10}), 140.6 (m, C_{PFP}), 139.6 (s), 139.3 (tr, C_{PFP}), 136.64 (m, C_{PFP}), 134.8 (br, C_{PFP}), 131.0 (br, C_{PFP}), 130.0 (s, 1C_b), 127.8 (s, 2$C_{8,12}$), 126.1 (s, 2$C_{7,13}$), 124.8 (d, $^3J_{C-F}$ = 14.5 Hz, C_e and C_f), 124.0 (s, $C_{g\ or\ d}$), 121.8 (s, $C_{g\ or\ d}$), 121.6 (br, C_3 and C_{17}), 117.34 (s, 2C_2 and C_{18}), 113.84 (m, C_{PFP}), 104.4(s, 1C_a). MALDI-TOF (M + H^+): m/z 762.62 (calcd), 763.17 (obsd). Anal. Calcd for $C_{35}H_{14}N_4SF_{10}$: C, 58.99; H, 1.98; N, 7.86; S, 4.50. Found: C, 59.80; H, 2.10; N, 7.92; S, 4.53. λ_{abs} (CH_2Cl_2, log ε = 5.04) = 421 nm. Φ_F = 0.004.

General Procedure for the Preparation of Oxocorrolatochromium-(V) Species. A detailed synthesis of oxocorrolatochromium species was adapted from a report in the literature.[20] Chromium hexacarbonyl (excess) was added to 20 mL of a boiling toluene solution of a free-base corrole (~45 mg). The reaction mixture was stirred for 2 h, during which time the solution changed from green (reactant) to reddish-brown (product). Product formation was also monitored by TLC assay. After cooling to room temperature, the crude mixture was filtered using a water aspirator to remove an excess of chromium hexacarbonyl crystals. The remaining toluene was removed by rotary evaporation. The dry crude product was then dissolved in a minimum volume of dichloromethane and purified by silica gel column chromatography (CH_2Cl_2/hexane). The blood-red fraction containing the oxochromium(V) species was collected. Subsequent recrystallization afforded a pure compound. Detailed crystallization systems for individual compounds are given below.

Synthesis of Oxo[5,15-bis(pentafluorophenyl)-10-(2-thienyl)-corrolato]chromium(V), [2THC Cr^VO] (1a). Recrystallization of complex **1a** from CH_2Cl_2/hexane afforded a pure compound. Yield: ~70%. MALDI-TOF (M^+): m/z 777.53 (calcd), 777.24 (obsd). λ_{abs} (CH_2Cl_2, log ε = 4.87) = 402 nm.

(21) Laha, J. K.; Dhanalekshmi, S.; Taniguchi, M.; Ambroise, A.; Lindsey, J. S. *J. Org. Process Res. Dev.* **2003**, *7*(6), 799–812.

(22) (a) Simkhovich, L.; Galili, N.; Saltsman, I.; Goldberg, I.; Gross, Z. *Inorg. Chem.* **2000**, *39*, 2704–2705. (b) Gryko, D. T.; Koszarna, B. *Org. Biomol. Chem.* **2003**, *1*, 350–357.

(23) Quantum yields were calculated using fluorescein as a reference.

Synthesis of Oxo[5,15-bis(pentafluorophenyl)-10-(3-thienyl)-corrolato]chromium(V), [3THC Cr^{V}O] (2a). Dark-red crystals of complex **2a** were obtained by recrystallization from CH_2Cl_2/hexane. Yield: ~70%. MALDI-TOF (M^+): m/z 777.53 (calcd), 777.18 (obsd). λ_{abs} (CH_2Cl_2, log ε = 4.86) = 403 nm.

Synthesis of Oxo[5,15-bis(pentafluorophenyl)-10-(3-thianaphthyl)-corrolato]chromium(V), [TNPC Cr^{V}O] (3a). A dark-red solid material signifying complex **3a** was obtained by recrystallization from CH_2Cl_2/hexane. Yield: 98%. MALDI-TOF (M^+): m/z 827.62 (calcd), 827.21 (obsd). λ_{abs} (CH_2Cl_2, log ε = 4.80) = 404 nm.

Synthesis of Oxo[5,10,15-tris(pentafluorophenyl)corrolato]-chromium(V) (4a). This compound has been previously prepared in the literature[20] and was resynthesized for comparison in these studies.

Synthesis of Oxo(5,10,15-tri-3-thienylcorrolato)chromium(V) (5a). Dark-violet crystals of complex **5a** were obtained by recrystallization from CH_2Cl_2/hexane. Yield: 37 mg, ~70%. MALDI-TOF (M^+): m/z 609.12 (calcd), 609.71 (obsd). λ_{abs} (CH_2Cl_2, log ε = 4.64) = 407 nm.

Synthesis of 5,15-Bis(pentafluorophenyl)-10-(3-thienyl)corrolato-copper(III), [3THC Cu] (2b). Copper(II) acetate monohydrate (excess) was added to a 10 mL volume of a pyridine solution of [3THC] (**2**; 40 mg, 0.056 mmol). The reaction mixture was stirred for ~2 h at room temperature. The crude reaction mixture was filtered directly through a pad of silica gel (CH_2Cl_2). The first brown fraction was collected and purified through the use of flash column chromatography (silica; CH_2Cl_2/hexane, 1:1). Solvent evaporation afforded a violet-red solid of **2b**. Yield: 30.5 mg, ~70%. MALDI-TOF ($M + H^+$): m/z 773.9 (calcd), 774.9 (obsd). λ_{abs} (CH_2Cl_2, log ε = 4.94) = 402 nm.

Crystallographic Studies. X-ray diffraction measurements were performed at 293 K with a Bruker SMART 1K CCD diffractometer using graphite-monochromated Mo Kα radiation (λ = 0.710 73 Å). Cell parameters were determined and refined by the *SMART* program.[24] Data reduction was performed through the use of *SAINT* software.[24] The data were corrected for Lorentz and polarization effects. An empirical absorption correction was applied using the *SADABS* program.[25] All intensity data were corrected for Lorentz and polarization effects. The structures were solved by direct methods using the program *SHELXS-974* and refined by full-matrix least-squares calculations (F^2) by using *SHELXL-97* software.[26] All non-H atoms were refined anisotropically against F^2 for all reflections. All H atoms were placed at their calculated positions and refined isotropically. Crystal data for compounds **1** and **2b** are given in Table 1. Selected bond lengths and angles for **2b** are listed in Table 2. The CIF files were deposited with the Cambridge Crystallographic Data Centre, and the following codes were allocated: CCDC 684998 (**1**) and 720659 (**2b**). These data can be obtained free of charge via the Internet at www.ccdc.cam.ac.uk/data_request/cif.

Results and Discussion

Synthesis. The corrolate synthesis was initiated by the preparation of dipyrromethane via $InCl_3$-catalyzed condensation conditions.[21] Then, a one-pot acid-catalyzed condensation, followed by DDQ oxidation, afforded the *meso*-A_2B free-base corrole[22b] through which the 5-/15-*meso*-aryl groups are derived from those of aryldipyrromethane. The [Cr=O] moiety was formally incorporated into the corrole through aerobic metallation of $Cr(CO)_6$ to give the respective chromium(V) species **1a**−**5a** (Scheme 2). Corrole resistance to oxidation occurs via such metallation. The Cu^{3+} complex **2b** and A_3-type compounds **4** and **4a**[21,22a] were also prepared to facilitate data comparison.

X-ray Crystallography. We have undertaken single-crystal X-ray diffraction studies of the free-base corrole **1** and the copper(III) corrolate species **2b** (Table 1 and the Supporting Information). Suitable single crystals for the X-ray diffraction study of **1** were obtained from a CH_2Cl_2/hexane (1:2) solvent mixture. The compound crystallized in the monoclinic space group $P2_1/n$. The structure of **1** (Figure 1a) confirms the existence of the

Table 1. Crystal Data for Compounds **1** and **2b**

	1	**2b**
empirical formula	$C_{35}H_{14}F_{10}N_4S$	$C_{35}H_{11}CuF_{10}N_4S$
fw	712.56	773.08
temperature (K), wavelength (Å)	243(2), 0.710 73	293(2), 0.710 73
cryst syst, space group	monoclinic, $P2_1/n$	monoclinic, $P2_1/n$
unit cell dimens		
a (Å)	14.4873(18)	14.9807(11)
b (Å)	7.7533(8)	10.7772(7)
c (Å)	25.313(3)	18.7525(13)
β (deg)	95.370(2)	100.179(5)
Vol (Å^3)	2830.8(6)	2979.9(4)
Z	4	4
density (calcd, Mg/m^3)	1.672	1.723
abs coeff (mm^{-1})	0.217	0.901
F(000)	1432	1536
cryst size (mm^3)	0.15 × 0.15 × 0.02	0.20 × 0.10 × 0.10
θ range for data collection	1.34−19.34	1.61−20.49
reflns colld	14 505	13 394
indep reflns	6390 [R(int) = 0.0846]	6390 [R(int) = 0.0846]
abs corrn	empirical	empirical
max and min transmn	0.9957 and 0.9682	0.8403 and 0.9153
data/restraints/param	6390/0/448	6390/0/448
GOF on F^2	0.979	1.071
final R indices [$I > 2\sigma(I)$]	R1 = 0.0736, wR2 = 0.1068	R1 = 0.0502, wR2 = 0.0970
R indices (all data)[a]	R1 = 0.2125, wR2 = 0.2275	R1 = 0.1236, wR2 = 0.1622

[a] $R1 = (\sum||F_o| - |F_d||)/\sum|F_o|$; $wR2 = [(\sum(F_o^2 - F_c^2)^2)/\sum w(F_o^2)^2]^{1/2}$.

Table 2. Comparative Selected Bond Lengths [Å] and Angles [deg] for Copper(III) Corrolate Complexes

	3THC(cor)Cu^{III} (**2b**)	tris(2TH)(cor)Cu^{III}[a]
	Bond Lengths	
N(1)−Cu(1)	1.888(6)	1.888(5)
N(2)−Cu(1)	1.894(6)	1.891(4)
N(3)−Cu(1)	1.907(6)	1.886(2)
N(4)−Cu(1)	1.873(6)	1.889(4)
	Bond Angles	
N(4)−Cu(1)−N(2)	166.9(3)	168.28(16)
N(1)−Cu(1)−N(3)	169.1(3)	168.40(16)

[a] Reference 18b. [b] The plane of the macrocycle is defined by the four pyrrolic N atoms.

(24) *SMART and SAINT, Area Detector Software Package and SAX Area Detector Integration Program*; Bruker Analytical X-ray: Madison, WI, **1997**.

(25) *SADABS, Area Detector Absorption Correction Program*; Bruker Analytical X-ray: Madison, WI, 1997.

(26) Sheldrick, G. M. *SHELXL-97*; Universität Göttingen: Göttingen, Germany, **1999**.

Scheme 2. Synthesis of A_2B-metallocorroles from Commercially Available Starting Materials

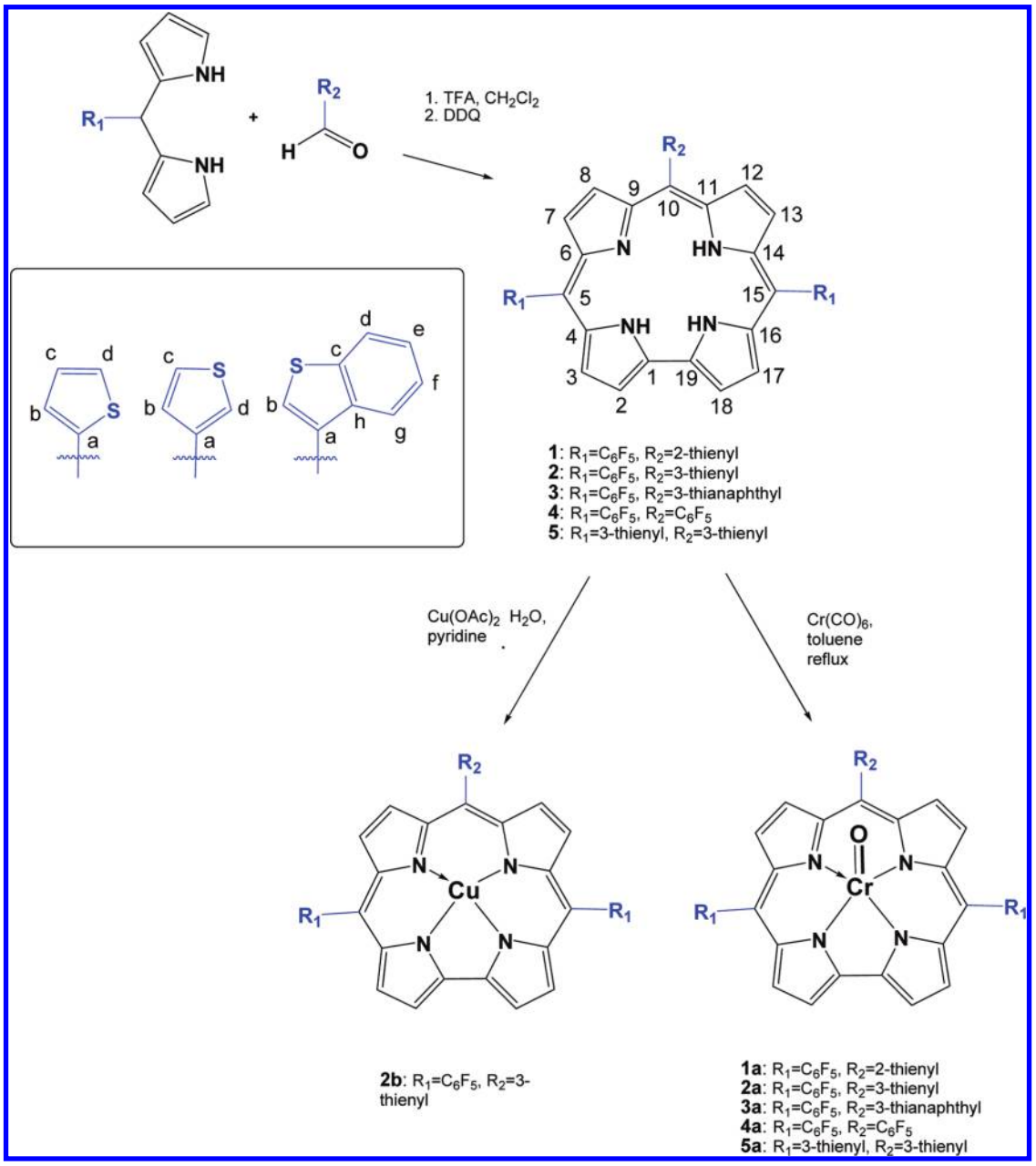

expected three *meso*-aryl groups and four constituent pyrrolyl groups, which are non-coplanar with the mean macrocyclic plane: one is bent downward, while another is bent upward. The *meso*-aryl groups are located toward the corrole core with dihedral values of ~121°. For the thienyl group, there is a ~124° dihedral angle value, signifying a slightly greater rotational flexibility for this moiety.[18b]

X-ray-diffraction-quality single crystals of **2b** were obtained via the slow evaporation of a CH_2Cl_2/hexane (1:1) mixture under ambient conditions. The molecular structure is consistent with the expected major synthetic product. The copper center adopts a distorted square-pyramidal environment in which four corrole N atoms occupy the equatorial position and the metal occupies the axial position (Figure 1b). The Cu−N bond lengths of **2b** are in the range of 1.873−1.907 Å, comparable with previously published data for, e.g., 5,10,15-tri-2-thienylcorrolatocopper(III) (Table 2). The structure of **2b**, in comparison with the oxochromium(V) species, does not possess out-of-[N_4]-plane metal atom displacement (vide infra).[20] Macrocyclic puckering is evident generally for the corroles, especially in the structure for **1**, in which the pyrrolyl ring mean planes are clearly non-coplanar with the corrole [N_4] mean plane.

While there are many literature examples available for comparison of the copper-containing structure of **2b** (refer to the Cambridge Structural Database), a very recent and intriguing report by Ghosh et al. focuses on the phenomenon of copper corrolate saddling.[1b] In this paper, it is asserted that "copper corroles are inherently nonplanar, even in the absence of sterically hindered substituents" because of Cu d−cor π orbital interactions. Indeed, there is a semblance of saddeling for derivative

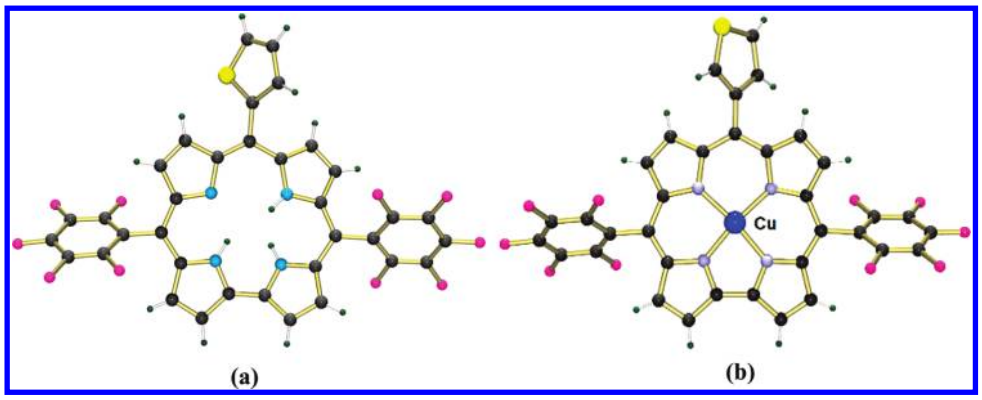

Figure 1. Crystal structures of compounds **1** (a) and **2b** (b).

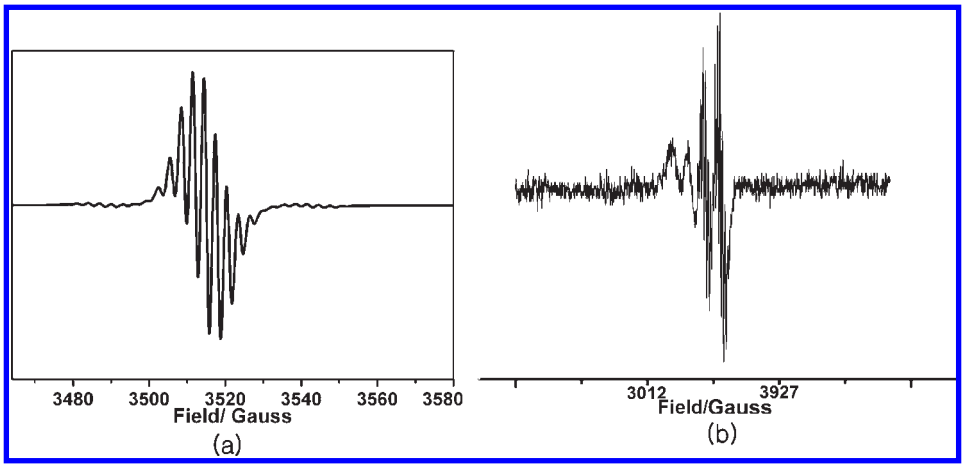

Figure 2. (a) EPR spectrum of **2a** in CH_2Cl_2 at 298 K. (b) EPR spectrum of **2b** upon the addition of 4 equiv of $NaBH_4$ in CH_2Cl_2 at 298 K. The microwave frequency, power, and modulation amplitude were 9.768 MHz, 5.0 mW, and 1.00 G, respectively.

2b, which can be appreciated when looking along the approximate *trans*-[N−Cu−N] vector, whereupon the distal ends of the pyrrolyl are clearly seen to bow to the same side away from the copper center. A greater version of analysis considering all pyrrolyl mean planes for all structurally known copper corrole species would be in order at a later time, to more comprehensively analyze the extent of saddling per peripheral substitution.

Unfortunately, suitable single crystals of the oxochromium(V) species **1a**−**4a** were not obtained. However, the X-ray diffraction study of *meso*-ABC-oxochromium(V) corrolate species has recently been published,[18e] demonstrating a relatively larger displacement (0.58 Å) of the Cr atom from the center of the tetrapyrrolyl macrocycle and exhibiting shorter Cr−N bond distances in line with strong σ donation from the N atoms of the corrole ring to the central metal atom (Table 2). This is in accordance with an enhanced benchtop stability found for the oxochromium(V) complexes.

EPR Study. The room temperature EPR spectra of oxochromium(V) species **1a**−**3a** and **5a** in dichloromethane display a sharp isotopic signal at g_0 around 1.98, confirming a $3d_{xy}^1$ ground-state electronic configuration for the oxochromium(V) complex. This signal is split into nine lines attributable to the coupling of the unpaired electron with four equivalent ^{14}N nuclei whose nuclear spin is 1 ($I = 1$); there are also satellite signals due to primary coupling with the less abundant ^{53}Cr nucleus, which possesses a spin of $^3/_2$ (9.5% abundance; Figure 2 and the Supporting Information). The isotropic hyperfine coupling constants of **1a**−**3a** and **5a** were obtained via computer simulation; these values are summarized in Table 3 and are presently compared with data of known literature compounds. The data of these new compounds fall within the range of those found for other corrole chromium(V) species, e.g., oxo[5-(4-bromophenyl)-10-(pentafluorophenyl)-15-(2-thianaphthyl)corrolato]chromium(V).[18e]

Table 3. EPR Parameters for the Series of Oxochromium(V) Corrole Complexes

complex	g_{iso}	$A_{^{53}Cr}$/mT	$A_{^{14}N}$/mT	ref
1a	1.986	1.61	0.30	this work
2a	1.985	1.62	0.30	this work
3a	1.988	1.61	0.30	this work
5a	1.988	1.55	0.30	this work
[ABC](cor)Cr^VO	1.989	1.59	0.30	18e
tris(pfp)(cor)Cr^VO	1.986	1.64	0.30	20
tris(pfp)(cor)Cr^VN		2.67	0.27	27a
tris(pfp)(cor)Cr^V(NAr)	1.987	2.18	0.31	27b
tris(pfp)(cor)Cr^V(NMes)	1.985	2.18	0.31	27b

The hyperfine coupling constants of oxochromium(V) species reflected a relative spin density of metal (low) and ligand (high), which have previously been rationalized via a strong N → M σ donation, followed by transfer of that density to the axial ligand by way of π donation.[20] In the

(27) (a) Golubkov, G.; Gross, Z. *Angew. Chem., Int. Ed.* **2003**, *42*, 4507–4510. (b) Edwards, N. Y.; Eikey, R. A.; Loring, M. I.; Abu-Omar, M. M. *Inorg. Chem.* **2005**, *44*, 3700–3708.

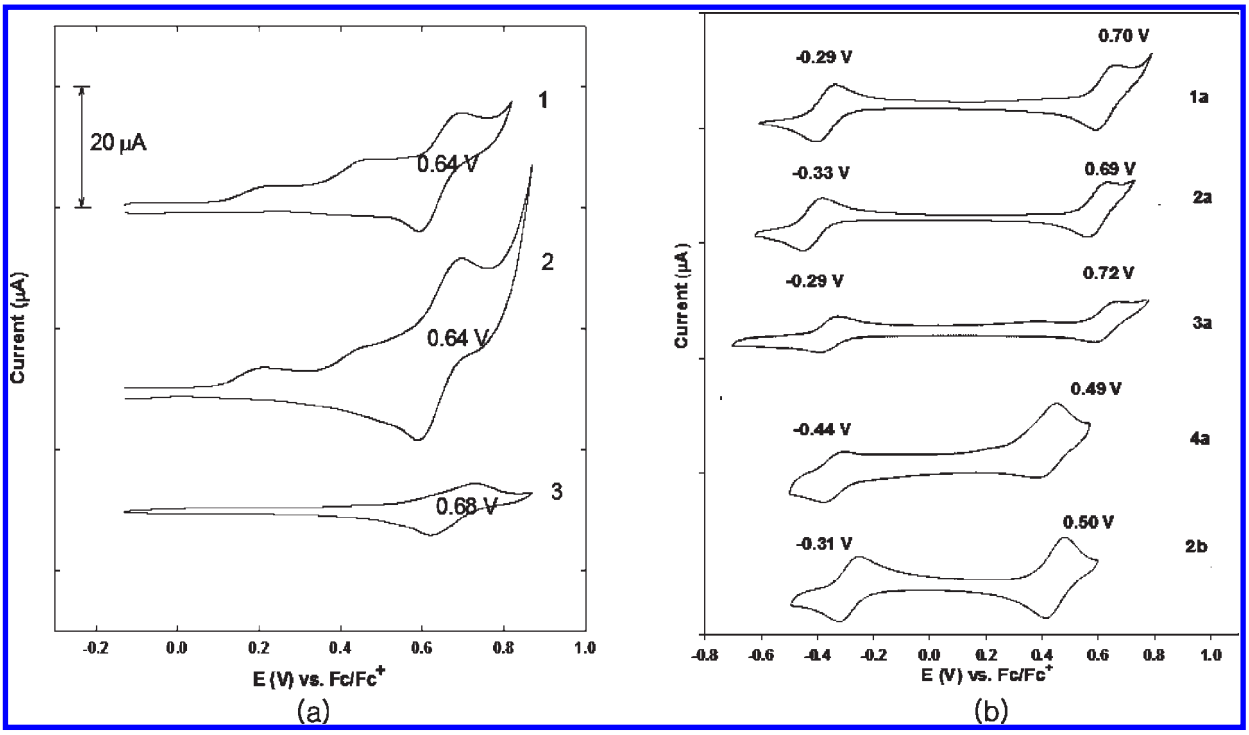

Figure 3. (a) Cyclic voltammograms of **1**−**3** in acetonitrile (1 mM) with 0.1 M TBAP. (b) Cyclic voltammograms of **1a**, **2a**, **2b**, **3a**, and **4a** in acetonitrile (1 mM), with 0.1 M TBAP at a scan rate of 100 mV/s (only second scans are provided). $E_{1/2}$ (V) values are provided for each species.

case of closely related nitrido[27a] and imido[27b] complexes, a similar situation exists, but in these cases, the strong π-donating ability of the axial ligand somewhat negates the σ-donating effect of pyrrolic N atoms; the relative spin density is thus much higher on the metal.

The $A_{^{14}N}$ coupling constant, reflecting the order of σ donation of the pyrrolic N atoms to the metal is greatest for the oxo species; this leads to the observed short metal−nitrogen pyrrole distances. These facts, together with the presence of a larger metal atom displacement from the plane of corrole macrocycle observed for $Cr^{V}O$ and $Cr^{V}N$ complexes (Table 3) when compared to non-axially ligated systems, are the main factors for stabilization of these complexes. Table 3 shows that the value of (^{53}Cr) decreases upon going from the strong tris-(C_6F_5)corrole electron-withdrawing ligand to **1a**−**3a** and finally to the tri-3-thienylcorrole (**4a**). This variation corresponds with the fact that the electronegativity of the meso substituents of the corrole ring decreases the electron density on chromium(V) and makes the π-bonding character of the $Cr^{V}=O$ moiety stronger.[28]

Also, EPR studies were pursued to confirm the high-oxidation-state nature of copper(III) in **2b**. The Cu^{3+} ion with a low-spin d^8 configuration is EPR-silent but, under treatment by $NaBH_4$, copper(II), which has an intense EPR signal and possesses a spin of $^1/_2$, can be seen to form (d^9, $I = {}^1/_2$)[29] (Figure 2b).

Electrochemistry. The cyclic voltammograms of corrole ligands **1**−**3** and their corresponding chromium complexes **1a**−**4a** have been obtained, and their redox potentials are also provided (Figure 3 and the Supporting Information). In the case of metal complexes, there are two one-electron reversible redox processes: a ligand-based oxidation corresponding to the corrole/corrole π-radical cation (ligand/ligand$^{\bullet+}$) couple and a metal-based reduction corresponding to the metal^n/metal^{n-1} couple.

One-electron oxidation potentials of thienyl- and thianaphthyl-containing free-base corroles are similar to each other and can be compared with tri-2-thienyl- and tri-3-thienyl-*meso*-A_3-corroles;[18b] the electrochemical oxidation potentials of **1** and **3** are positively shifted by ~0.5 V. This observation can be explained in terms of a difference of the electron-withdrawing strength of meso substituents in the corrole ring. This notion corresponds to the oxidation potentials of oxochromium(V) complexes **1a**−**3a**, which demonstrate quite similar values for the thienyl- and thianaphthyl-containing ligands, but in the case of the tri-3-thienylcorrole ligand (**4a**), its oxidation potential is negatively shifted by ~0.2 V.

A comparison of the electrochemical measurements between the Cu^{III}-containing compound **2b** and tri-3-thienylcorrole[18b] shows that the oxidation potential for the ligand with two C_6F_5 groups is positively shifted by 0.23 V [0.50 vs 0.23 V, Fc/Fc$^+$, for **2b** and tri-3-thienylcorrolatocopper(III), respectively], also consistent with patterns of the substituent electron-withdrawing capacity.

The reduction potential of the oxochromium(V) species **1a**−**4a** can be discussed, together with the catalytic activity of obtained compounds in oxygen-transfer reactions; its mechanism suggests a reduction of Cr^{V} and oxidation of organic substrates.[30] The less positive $Cr^{V}O/Cr^{VI}$

(28) Fujii, H.; Yoshimura, T.; Kamada, H. *Inorg. Chem.* **1997**, *36*, 1122–1127.

(29) Fox, J. P.; Ramdhanie, B.; Zabera, A. A.; Czernuszewicz, R. S.; Goldberg, D. P. *Inorg. Chem.* **2004**, *43*, 6600–6608.

(30) Mahammed, A.; Gray, H. B.; Meier-Callahan, A. E.; Gross, Z. *J. Am. Chem. Soc.* **2003**, *125*, 1162–1163.

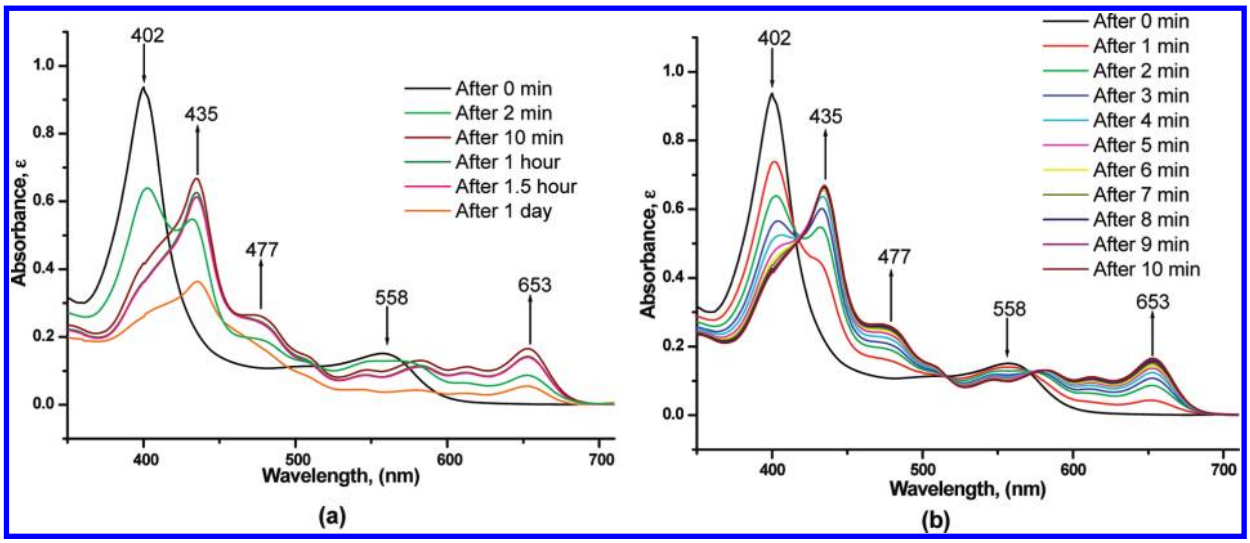

Figure 4. (a) Time-dependent UV−vis spectra of **1a** during aerobic oxidation of PPh_3 to $O{=}PPh_3$ in MeCN with the addition of 0.7% pyridine. (b) UV−vis spectra of the oxidation of PPh_3 to $O{=}PPh_3$ during the first 10 min. See ref 18e for comparison with a closely related *meso*-ABC-corrolate.

potential supports a prediction of low catalytic activity for the oxochromium(V) species. From this perspective, a higher catalytic ability is suggested for the **1a** and **3a** oxochromium(V) species, owing to a slightly higher positive reduction potential than that for **2a** and a much higher positive reduction potential than that for **4a**. Thus, the presence of relatively weak electron-withdrawing groups, such as thienyl, at the periphery of the corrole core, decreases the reduction potential of the Cr^V/Cr^{IV} couple and, consequently, worsens the catalytic ability of oxochromium(V) species toward oxidation of organic substrates.

Catalytic Reactivity of Oxochromium(V) Species. We have examined the catalytic activity of the oxochromium(V) species **1a** toward PPh_3 in acetonitrile. Acetonitrile was chosen as the solvent because of the large solvent effect that increases the rate of the oxidation reaction.[30] Specifically, we observed an oxidation reaction of PPh_3 to $O = PPh_3$ in the presence of 0.7% pyridine, which inhibits reoxidation of Cr^{III} to Cr^V. The catalytic cycle in the reaction likely includes (i) reduction of Cr^V to Cr^{III} with additional coordination of two axial substrates and also (ii) formation of the Cr^{IV} dimer as an intermediate. UV−vis spectra (Figure 4) reflect that the catalytic reaction is immediate; the new peak appearing at $\lambda_{abs,max}$ of 435 nm corresponds to Cr^{IV}. A new shoulder at ~477 nm reflects a buildup in the concentration of Cr^{III}.[30] We can then suggest that the less electron-withdrawing groups on the periphery of the corrole ligand have a moderate effect on decreasing the catalytic strength of the oxochromium(V) species. These results can be best placed in context with respect to a previous comprehensive report by Gross and co-workers.[1c] The complexes studied involved chromium centers of closely related corrole complexes that form, or were prepared, in stepwise valence states:[1d] [(tpf)corCr(py)$_2$] (trivalent), [(tpf)corCr=O][Cp_2Co] (tetravalent), (tpf)corCr=O (pentavalent), and [[(tpf)cor$^•$]Cr=O][$SbCl_6$] (hexavalent). Also, with respect to the presence of the Cr=O bond and its oxidizing strength, there is the important consideration of the frequency and strength of the Cr=O bond. This has been nicely addressed by a recent report from Czernuszewicz and co-workers.[1e]

UV−Vis Spectroscopy and Titration of Free-Base Corroles and Oxochromium Complexes with Metal Ions. A UV−vis study for both the free-base corroles and metallocomplexes was carried out in methylene chloride because compounds are more stable in this solvent (see the solvent stability assays in the Supporting Information). Optical properties for all compounds are given in Table 4.

Emission and absorption spectra of sulfur-containing free-base corroles **1**−**4** were obtained upon the addition of perchlorate salts[32] of Cs^+, Na^+, K^+, Ag^+, Ca^{2+}, Mn^{2+}, Co^{2+}, Ni^{2+}, Zn^{2+}, Cu^{2+}, Cd^{2+}, and Pb^{2+}. Titration data of these show large absorption changes for the free-base corroles (Figure 5), with markedly less selectivity for Cu^{2+} (see the Supporting Information), demonstrating strong ligand−metal ion interactions. Solutions of compounds **1**−**3** changed from violet-green to light-green upon the addition of Cu^{2+}, Pb^{2+}, Hg^{2+}, and Cd^{2+}, with a decrease in $\lambda_{abs,max}$ and bathochromic shifting [415 → ~425 (**1**), 416 → ~421 (**2**), and 423 → ~433 (**3**)]; the respective "Q bands" also underwent red shifts: 561 → ~655 (**1**), 563 → ~657 (**2**), and 565 → 657 (**3**). The greatest decrease in the Soret band intensity for **1**−**3** occurred upon Cu^{2+} addition. New spectral shoulders formed at 445 (**1** and **2**) and 453 nm (**3**) upon the addition of Cu^{2+}, Pb^{2+}, Hg^{2+}, or Cd^{2+}, consistent with the general degree of thiophilicity of these metals. Deviation from direct corrole metallation may occur as a function of increased sulfur richness, wherein other minor coordination possibilities probably exist but have been pursued herein neither experimentally nor computationally.

Type III M^{n+} recognition was investigated by way of screening **1a**−**5a** with the same perchlorate salts[32] as those for free-base corroles. Solutions of **1a**−**3a** (=L) are not fluorescent, so only titrimetric UV−vis absorption data were obtained (Figure 6). Significantly, [Cu^{2+}] addition to **1a**−**3a** (1:1 M^{n+}/L) afforded a rapid, significant, and selective optical response (pink → red-brown;

(31) Ding, T.; Aleman, E. A.; Modarelli, D. A.; Ziegler, C. *Phys. Chem. A* **2005**, *109*, 7411–7417.
(32) Churchill, D. G. *J. Chem. Educ.* **2006**, *83*, 1798.

Table 4. Optical Properties for Free-Base and Metallocorrole Complexes[a]

compound	$\lambda_{abs,\ max}$ (nm)	log ε/(M^{-1} cm^{-1})	$\lambda_{em,max}$ (nm)	Stokes' shift [b] (cm^{-1})	ϕ_F [c]
1	415	5.20	631	519	0.003
2	416	5.10	657	1066	0.004
3	421	5.04	631	546	0.004
4[d]	407	4.51	642	1059	
1a	402	4.87			
2a	403	4.86			
3a	404	4.80			
4a[d]	402	4.91			
5a	407	4.64			
2b	402	4.94			

[a] Spectral properties in CH_2Cl_2 at room temperature. [b] Stokes' shifts were calculated from respective absorption and emission wavelengths. [c] Quantum yields were calculated using fluorescein dissolved in 0.1 N NaOH as a reference (ϕ = 0.93). [d] Published data.[20,31]

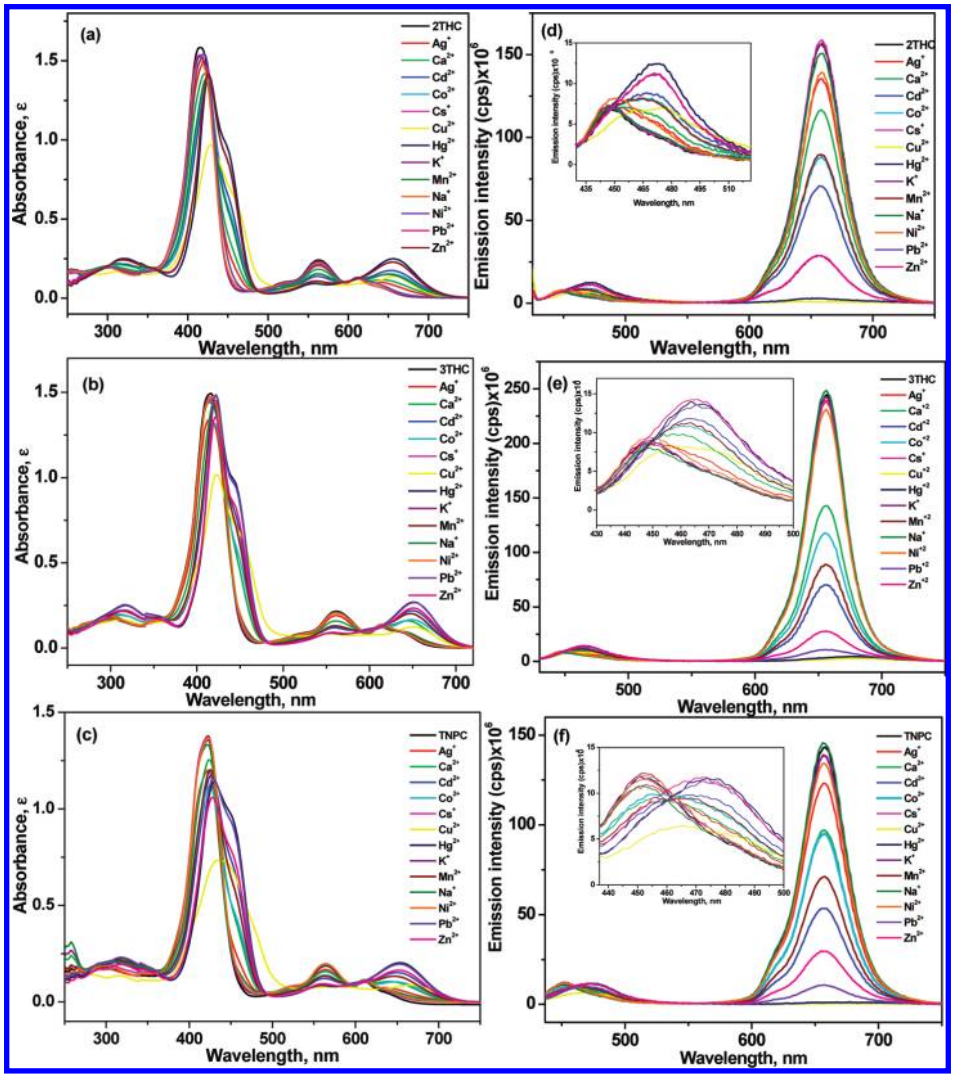

Figure 5. Changes of the absorption spectra of (a) **1**, (b) **2**, and (c) **3** and emission spectra of (d) **1**, (e) **2**, and (f) **3** upon the addition of various metal ions. The ligand/metal ion ratio is 1:1. The concentration of the ligand in CH_2Cl_2 is 1×10^{-5} M, and that of the M^{n+} solution in CH_3CN is 1×10^{-3} M. Excitation wavelengths: 631 (**1**), 657 (**2**), and 631 nm (**3**).

Supporting Information). In the case of other metal ions, very little change was observed.

The observed Cu^{2+} selectivity prompted us to carry out titration experiments for **1a**−**3a** with $Cu(ClO_4)_2$ (Figure 7). The limit of quantification for [Cu^{2+}] in solutions of **1a**−**3a** was 1.0×10^{-5} M. The Job plot analysis confirmed 1:1 Cu^{2+}/L stoichiometry; K_a values for Cu^{2+} (**1a**, 6.9×10^4 M^{-1}; **2a**, 8.6×10^4 M^{-1}; **3a**, 6.9×10^4 M^{-1}) were obtained using the Benesi−Hildebrand equation. These similar values support the same proposed mode of binding, i.e., via the terminal oxo group, i.e., [M═O···Cu^{2+}].

To pursue a fuller understanding of the *meso*-A_2B-oxocorrolate of chromium(V) and the nature of M^{n+} binding, we have considered comparisons between additional corrolato species (the $Cr^{V}O$-free moiety, **2b**; the "S-free" version, **4a**; the C_6F_5-free version, **5a**) and have

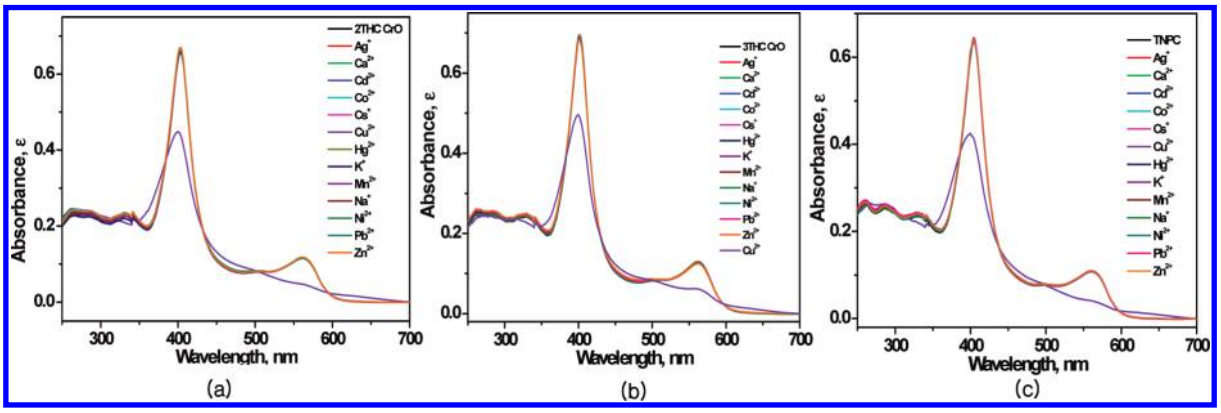

Figure 6. Changes of the absorption spectra of (a) **1a**, (b) **2a**, and (c) **3a** upon the addition of various metal ions. The ligand/metal ion ratio is 1:1. The concentration of the ligand in CH_2Cl_2 is 1×10^{-5} M, and that of the M^{n+} solution in CH_3CN is 1×10^{-3} M.

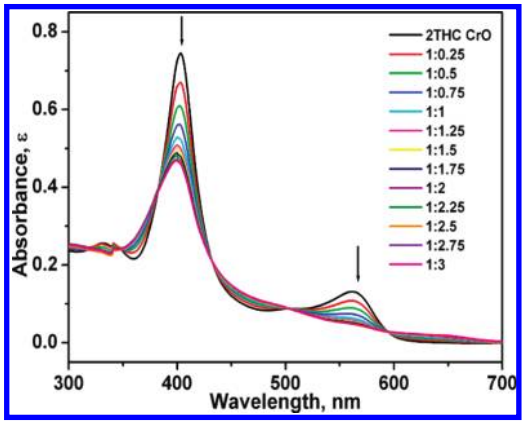

Figure 7. UV−vis titration spectrum obtained by titration of a Cu^{2+} solution in CH_3CN to a solution of **1a** (1×10^{-5} M) in CH_2Cl_2.

carried out a series of experiments (UV−vis, CV, and EPR spectroscopy; see the Supporting Information). Solutions of **2b**, **4a**, and **5a** were treated with various mono- and divalent metal ions for obtaining a 1:1 ratio of L (**2b**, **4a**, and **5a**): M^{n+} in solution (Supporting Information). In comparison, through the use of UV titration data of **1a**−**3a**, it should be noted that the S-free (**4a**) and $Cr^{V}O$-free species (**2b**) also possess selectivity to cupric ions, but in the case of **4a**, the intensity of the Soret band decreases with a retention of the Q-band maximum upon the addition of Cu^{2+}. The spectrum of the $Cr^{V}O$-free corrole (**2b**) possesses a sizable diminution of the Soret band. These changes are comparable with the transformations of **1a**−**3a** upon Cu^{2+} addition. UV-titration data of **5a** revealed a significant interaction of the compound with divalent ions, particularly upon treatment with Hg^{2+} and Cu^{2+} (the Soret band disappears; new $\lambda_{abs,\ max}$ = 460 nm) and Cd^{2+} and Pb^{2+} [the intensity of the Soret band decreases considerably; new $\lambda_{abs,\ max}$ = ∼460 nm (Pb^{2+}) or a shoulder (Cd^{2+}) forms]. Additionally, we titrated **5a** by Cu^{2+}, Hg^{2+}, Pb^{2+}, and Cd^{2+} separately for a final analysis of the behavior of **5a** upon the addition of excess metal ion (Supporting Information). Titration data for **5a** by Cd^{2+} did not show large spectral changes: the intensity of the Soret band decreased slightly; new shoulders at ∼460 and 625 nm did form. For the Cu^{2+}, Hg^{2+}, and Pb^{2+} titrations, the spectrum of **5a** transformed dramatically: the Soret band disappeared completely, with a new concomitant absorption band arising at ∼460 nm. These data indicate a vastly different nature of interaction of **5a** with Cd^{2+} versus **5a** with Cu^{2+}, Hg^{2+}, and Pb^{2+}. In the latter case, a significant reconfiguration occurred at the sensing molecule, suggestive that displacement of the $Cr^{V}O$ moiety has occurred. To investigate the M^{n+} binding further, stoichiometry and K_a values were obtained (Job plot and Benesi−Hildebrand methods, respectively). In all cases, L/M^{n+} binding stoichiometry was 1:1, except for Hg^{2+}, which reflects a 1:2 binding ratio (see the Supporting Information). Thus, taking all of the observations above together allow us to suggest that (i) the contribution of the $Cr^{V}O$ moiety and the thienyl group S atom could be operating together in varying degrees in metal ion chelation and thus in metal recognition and (ii) the combination of one thienyl group with two C_6F_5 rings allows for the retention of Cu^{2+} selectivity. Accordingly, the structure of the thienyl *meso*-A_2B oxocorrolates of chromium(V) is more effective as a potential sensor when compared to A_3 compounds (**4a** and **5a**) or to the copper complex (**2b**).

Conclusion

Herein, we provide the first examples of thienyl-*meso*-A_2B- and A_2B-oxochromium(V) corrolates, which have been prepared by standard methods and characterized by techniques that include EPR spectroscopy, single-crystal X-ray diffraction, CV, UV−vis, and 2D NMR spectroscopy. This paper also delineates three potential detection types (types I−III). Rapid and selective type III ($M{=}O\cdots M^{n+}$) detection was fruitful for Cu^{2+}, known for its biological role in neurodegeneration. The M=O group in porphyrin-(*un*)like systems has been carefully considered as the active portion of the real "compound I" or in structural/reactive mimics of it.[1] While chromium was explored here, studies of more metal-containing systems will help broaden the understanding of type II sensing capabilities. A type I detection potential was also catalogued herein, whereas results pertaining to a type II detection potential were briefly discussed only (Scheme 1). We emphasize the potential in integrating detection "types I−III", which should prove very interesting, based on the many previous *catalytic* investigations of corroles reported so far. Subtleties of type I−III optics can be addressed through future theoretical calculations as well.

Acknowledgment. D.G.C. acknowledges support from the Korea Science and Engineering Foundation (KOSEF;

Grant R01-2008-000-12388-0) and the National Research Foundation of Korea (Grant N01090203). O.A.E. was supported in the Molecular Logic Gate Laboratory by a BK-21 postdoctoral fellowship. J.K. acknowledges support from the Nano/Bio Science & Technology Program (Grant 2005-01333) of the Ministry of Education, Science and Technology. Hack Soo Shin helped greatly in acquiring NMR spectroscopic data. Teresa Linstead (CCDC) is acknowledged for aiding in the structural data deposition.

Supporting Information Available: Details of syntheses, NMR and UV−vis spectra, additional discussion, CV plots, EPR spectra, and crystallographic data in CIF format. This material is available free of charge via the Internet at http://pubs.acs.org.